Chinese Journal of Natural Medicines

Rehmanniae Radix Praeparata aqueous extract improves hepatic ischemia/reperfusion injury by restoring intracellular iron homeostasis

Yinhao ZHANG, Kexin JIA, Yufei LI, Zhi MA, Guifang FAN, Ranyi LUO, Yajing LI, Yang YANG, Fanghong LI, Runping LIU, Jia LIU, Xiaojiaoyang LI

Citation: Yinhao ZHANG, Kexin JIA, Yufei LI, Zhi MA, Guifang FAN, Ranyi LUO, Yajing LI, Yang YANG, Fanghong LI, Runping LIU, Jia LIU, Xiaojiaoyang LI, Rehmanniae Radix Praeparata aqueous extract improves hepatic ischemia/reperfusion injury by restoring intracellular iron homeostasis, Chinese Journal of Natural Medicines, 2024, 22(9), 769−784. doi: 10.1016/S1875−5364(24)60719−3.

View online: https://doi.org/10.1016/S1875−5364(24)60719−3

Available online at www.sciencedirect.com
ScienceDirect
Chinese Journal of Natural Medicines 2024, **22**(9): 769-784
doi: 10.1016/S1875-5364(24)60719-3
Chinese Journal of Natural Medicines

•Original article•

Rehmanniae Radix Praeparata aqueous extract improves hepatic ischemia/reperfusion injury by restoring intracellular iron homeostasis

ZHANG Yinhao[1], JIA Kexin[1], LI Yufei[2], MA Zhi[1], FAN Guifang[2], LUO Ranyi[1], LI Yajing[1], YANG Yang[2], LI Fanghong[2], LIU Runping[2], LIU Jia[1], LI Xiaojiaoyang[1*]

[1] *School of Life Sciences, Beijing University of Chinese Medicine, Beijing 100029, China;*
[2] *School of Chinese Materia Medica, Beijing University of Chinese Medicine, Beijing 100029, China*

Available online 20 Sep., 2024

[ABSTRACT] Hepatic ischemia/reperfusion injury (HIRI) is a common pathophysiological condition occurring during or after liver resection and transplantation, leading to hepatic viability impairment and functional deterioration. Recently, ferroptosis, a newly recognized form of programmed cell death, has been implicated in IRI. Rehmanniae Radix Praeparata (RRP), extensively used in Chinese herbal medicine for its hepatoprotective, anti-inflammatory, and antioxidant properties, presents a potential therapeutic approach. However, the mechanisms by which RRP mitigates HIRI, particularly through the regulation of ferroptosis, remain unclear. In this study, we developed a HIRI mouse model and monocrotaline (MCT)- and erastin-induced *in vitro* hepatocyte injury models. We conducted whole-genome transcriptome analysis to elucidate the protective effects and mechanisms of RRP on HIRI. The RRP aqueous extract was characterized by the presence of acteoside, rehmannioside D, and 5-hydroxymethylfurfural. Our results demonstrate that the RRP aqueous extract ameliorated oxidative stress, reduced intracellular iron accumulation, and attenuated HIRI-induced liver damage. Additionally, RRP significantly inhibited hepatocyte death by restoring intracellular iron homeostasis both *in vivo* and *in vitro*. Mechanistically, the RRP aqueous extract reduced intrahepatocellular iron accumulation by inhibiting ZIP14-mediated iron uptake, promoting hepcidin- and ferroportin-mediated iron efflux, and ameliorating mitochondrial iron aggregation through upregulation of Cisd1 expression. Moreover, siRNA-mediated inhibition of hamp synergistically enhanced the RRP aqueous extract's inhibitory effect on ferroptosis. In conclusion, our study elucidates the mechanisms by which RRP aqueous extracts alleviate HIRI, highlighting the restoration of iron metabolic balance. These findings position RRP as a promising candidate for clinical intervention in HIRI treatment.

[KEY WORDS] Hepatic ischemia/reperfusion injury; Rehmanniae Radix Praeparata; Ferroptosis; Intracellular iron homeostasis
[CLC Number] R965 **[Document code]** A **[Article ID]** 2095-6975(2024)09-0769-16

Introduction

Liver transplantation (LT) is a critical, life-saving procedure for approximately one million individuals worldwide suffering from end-stage liver diseases [1]. However, LT is associated with significant risks, including the potential for unpredictable intraoperative and postoperative complications, such as hepatic ischemia/reperfusion injury (HIRI). HIRI can lead to adverse clinical outcomes, complicating patient recovery [2]. HIRI typically progresses through two distinct phases: the acute ischemic anoxic phase and the secondary reperfusion injury phase [3]. During the ischemic anoxic phase, an imbalance in intracellular ATP production and mitochondrial dysfunction triggers the release of danger-associated molecular patterns (DAMPs) and reactive oxygen species (ROS), leading to the activation of Kupffer cells and subsequent short-term inflammation [4]. In the reperfusion phase, reoxygenation exacerbates the injury as excessive ROS production activates immune responses, causing increased hepatocyte death through apoptosis, necrosis, ferroptosis, and pyroptosis [5]. Currently, therapeutic options for patients with HIRI are limited to the use of ROS inhibitors, such as N-acetylcysteine (NAC), tiopronin, and silymarin. Consequently,

[Received on] 12-Nov.-2023
[Research funding] This work was supported by Beijing Nova Program (No. Z201100006820025), the National Natural Science Foundation of China (No. 82274186), the Fundamental Research Funds for the Central Universities (No. 2023-JYB-JBZD-046), the National High-Level Talents Special Support Program to LI Xiaojiaoyan, the National Key Research and Development Program on Modernization of Traditional Chinese Medicine (No. 2022YFC3502100), and Beijing Municipal Science & Technology Commission (No. 7212174).
[*Corresponding author] E-mail: xiaojiaoyang.li@bucm.edu.cn
These authors have no conflict of interest to declare.

there is an urgent need to develop new interventions to mitigate the risk of HIRI and improve patient outcomes following LT.

Ferroptosis is a newly identified form of iron-dependent cell death characterized by the intracellular accumulation of lipid peroxides and iron overload [6]. Since the liver is the primary organ responsible for maintaining iron metabolic homeostasis, ferroptosis has been closely linked to the development of various liver diseases [7]. Hepcidin (Hamp), a peptide hormone predominantly produced in hepatocytes, plays a central role in regulating iron homeostasis. Hypoxia and excessive inflammatory factors have been shown to influence hepcidin synthesis, thereby inhibiting the release of ferrous ions into the labile iron pool (LIP) [8]. Hepcidin also regulates ferroportin (FPN, *Slc40a1*), the sole cellular iron efflux protein, which results in the retention of iron in iron-exporting cells and affects systemic iron levels [9]. Additionally, solute carrier family 39 member 14 (ZIP14, *Slc39a14*) has been identified as a key mediator of ferroptosis by transporting non-transferrin-bound iron (NTBI) [8]. During ischemic and hypoxic conditions in the liver, ZIP14 expression is upregulated, and its transporter efficiency is enhanced by pro-inflammatory cytokines such as interleukin-1 (IL-1) [9]. Furthermore, the consumption and capacity of LIP are regulated by other critical proteins, including CDGSH iron sulfur domain 1 (CISD1, *Cisd1*), which influences mitochondrial iron homeostasis and ROS [10], and heat shock protein 1 (HSPB1), which decreases transferrin receptor (TFR-1) expression [11]. These findings indicate that a variety of ferroptosis-related proteins, such as hepcidin, FPN, ZIP14, CISD1, and HSPB1, play pivotal roles in iron homeostasis and the pathogenesis of HIRI. Nevertheless, further research is essential to fully elucidate these mechanisms and their implications.

Accumulating evidence supports the potential of traditional Chinese medicine (TCM) as a rich source for novel drug discovery. Rehmanniae Radix (RR), the tuberous root of dried *Rehmannia glutinosa*, was first documented in *Shennong's Classic of Materia Medica* [12] and is well-regarded in TCM for its liver-protective properties [13]. Rehmanniae Radix Praeparata (RRP, Shu-di-huang) is derived from dried RR through a process involving repeated steaming and drying cycles, and it has been widely utilized in clinical settings. Over 100 components have been isolated from RRP, primarily including cyclic ether terpenes and their glycosides, iridoid glycosides, and phenylethanoid glycosides [14]. RRP is known to exhibit anti-inflammatory and antioxidant effects by modulating cytokine levels such as IL-6, thereby demonstrating hepatoprotective properties [15]. Recent studies suggest that RRP may also mitigate ferroptosis, as its natural components have been shown to enhance the cysteine/glutathione peroxidase 4 (GPX4) pathway and regulate iron metabolism [13]. While inflammatory factors like IL-6 can exacerbate HIRI via the bone morphogenetic proteins/small mother against decapentaplegic (BMP/SMAD) pathway by affecting hepcidin expression and hepatocyte iron metabolism [16], it remains unclear whether RRP can confer hepatoprotective benefits and effectively improve HIRI by preventing ferroptosis and correcting iron metabolism imbalances in hepatocytes. This study aims to address this gap.

In this study, we first isolated and confirmed the quality of the aqueous extract of RRP. We then investigated the protective effects of RRP using an *in vivo* HIRI mouse model and *in vitro* monocrotaline (MCT)- and erastin-induced cell models. To uncover the underlying mechanisms of RRP against HIRI, we applied RNA sequencing for comprehensive bioinformatics analysis and employed molecular biology techniques to evaluate whether the protective effects of RRP were closely related to the reversal of ferroptosis. Collectively, our findings strongly suggest that RRP may be a promising therapeutic option for the treatment of HIRI and its complications by improving intracellular iron homeostasis.

Materials and Methods

Materials

MCT was obtained from Innochem Technology Co., Ltd. (Beijing, China). Erastin, ferrostatin-1 (Fer-1), and other reagents were sourced from Yuanye Bio-Technology Co., Ltd. (Shanghai, China). The antibody against ZIP14 (PA5-87880) was purchased from Thermo Scientific Co. (Massachusetts, USA). The antibody for hepcidin (sc-100277) was acquired from Santa Cruz Biotechnology (Santa Cruz, USA). The transferrin antibody (17435-1-AP) was sourced from Proteintech (Rosemont, USA), and the *β*-actin (4970S) was obtained from Cell Signaling Technology (Danvers, USA). Additional consumables for cell culture and flow cytometry analysis were procured from Sigma-Aldrich (St. Louis, USA).

Animal study

Eight-week-old male C57BL/6J mice (22−24 g) were obtained from SIBEIFU Biotechnology Co. (Beijing, China). The mice were maintained in a temperature-controlled environment (22 ± 2 ℃) with standard chow and sterile water available *ad libitum*, under a 12-hour light/12-hour dark cycle. They were randomly assigned to six groups (n = 6 per group): Sham group, HIRI group, HIRI + RRP low-dose (L, 2.5 g·kg^{-1}) group, HIRI + RRP medium-dose (M, 5 g·kg^{-1}) group, and HIRI + RRP high-dose (H, 10 g·kg^{-1}) group. RRP extract was administered by gavage for one week at different dosages depending on the group. Following pretreatment, mice were anesthetized with isoflurane, and a midline laparotomy was performed to expose the liver. Noninvasive microvascular forceps were used to clamp the portal vein and hepatic artery. The sham group (group 1) underwent the same surgical procedure without vascular occlusion. After 90 min of ischemia, the clamps were released to initiate a 6-hour reperfusion period. Upon completion, all liver and serum samples were collected immediately for further analysis. All

animal studies and procedures were approved by the Institutional Animal Protection and Use Committee of Beijing University of Traditional Chinese Medicine and conducted in accordance with relevant guidelines and regulations.

Biochemical analysis

Serum levels of alanine aminotransferase (ALT), aspartate aminotransferase (AST), lactate dehydrogenase (LDH), and nitric oxide (NO) were measured using specific kits: ALT (Nanjing Jiancheng, China, C010-2-1), AST (Nanjing Jiancheng, China, C009-2-1), LDH (Nanjing Jiancheng, China, A020-2-2), and NO (Beyotime Biotechnology, China, S0021S). The malondialdehyde (MDA) content in liver tissues was assessed using an MDA assay kit (Nanjing Jiancheng, China, A003-1). Glutathione (GSH) levels in BRL cells were determined using a GSH assay kit (Nanjing Jiancheng, China, A006-2-1). Total iron and ferrous ion concentrations in the medium supernatant were quantified with the total iron ion kit (Elabscience, China, E-BC-K772-M) and the ferrous ion kit (Elabscience, China, E-BC-K773-M).

Transmission electron microscope (TEM) and hematoxylin & eosin (H&E) staining

Liver tissues from different groups were fixed with 2.5% glutaraldehyde and mounted on formvar-carbon grids. After dehydration, maceration, and embedding, the samples were stained with a mixture of uranyl acetate and methyl cellulose for Transmission electron microscopy (TEM) analysis. Images were captured using a Zeiss Libra 120 transmission electron microscope (Carl Zeiss, Germany). For H&E staining, mouse liver tissues were fixed in 4% formaldehyde for 7 d, embedded in paraffin wax, and sectioned into 5 μm thick slices. The paraffin sections were then prepared for H&E staining as previously described, and images were captured using an Aperio Versa digital pathology scanner (Leica, Wetzlar, Germany).

RNA-sequencing analysis and quantitative real-time PCR (qPCR)

Total RNA from mouse liver tissues was extracted using Trizol reagent and quantified with a NanoPhotometer® spectrophotometer (IMPLEN, USA). mRNA was purified, and 250−300 bp cDNA fragments were enriched to create sequencing libraries on the Illumina Novaseq platform, following established protocols [17]. Gene expression data were normalized, and differentially expressed genes (DEGs) were identified using the edgeR package. Enrichment analysis of gene ontology (GO) terms and Kyoto Encyclopedia of Genes and Genomes (KEGG) pathways was performed using the clusterProfiler R package. Additionally, genomic enrichment analysis (GSEA) and heatmap visualization were utilized to further interpret the differential expression data. For the qPCR experiments, cDNA was synthesized from total RNA using the HiScript III RT SuperMix (R323-01, Vazyme Biotech). qPCR was conducted to quantify mRNA expression levels of target genes, with *Hprt1* used as the normalization control. Primer sequences for qPCR are available upon request from the corresponding author.

Cell culture and treatment

BRL hepatic cell lines were cultured in Dulbecco's Modified Eagle Medium (DMEM) supplemented with 10% fetal bovine serum and 1% penicillin/streptomycin at 37 °C in a 5% CO_2 atmosphere. RRP aqueous extracts were filtered through 0.8 and 0.22 μm Millipore filters, then diluted to final concentrations of 50, 100, and 150 $mg \cdot mL^{-1}$ in DMEM. MCT, which induces liver injury by blocking hepatic sinusoids, was used to mimic hepatocyte damage under HIRI conditions. Erastin, a known ferroptosis inducer, was employed to promote the accumulation of endogenous reactive oxygen species (ROS) and ferroptosis, serving as a positive control to explore the role of RRP aqueous extract in ferroptosis inhibition. For the experiments, BRL cells were pre-treated with RRP aqueous extract at concentrations of 50, 100, and 150 $\mu g \cdot mL^{-1}$ for 1 h. Subsequently, the cells were exposed to MCT (500 $\mu mol \cdot L^{-1}$) or erastin (10 $\mu mol \cdot L^{-1}$) for 24 h. Additionally, the ferroptosis inhibitor Fer-1 (1 $\mu mol \cdot L^{-1}$) was applied for 1 h following the 24-hour MCT or erastin treatment. The dosages for MCT, erastin, and Fer-1 were selected based on previous studies [18-20]. Following the treatments, cells were washed with PBS and collected for subsequent analyses. siRNAs targeting hamp and control siRNAs were designed and synthesized by Shanghai Hanbio Co., Ltd. (China). BRL cells, at 70%–90% confluence, were transfected with LipoFiter (HB-LF-1000) for 48 h. After transfection, the cells were treated with stimulators or RRP for an additional 12 h.

Flow cytometry

Hepatocyte apoptosis was assessed using the Annexin V (AV)/Propidium Iodide (PI) kit (C1067S, Beyotime, China) according to the manufacturer's instructions. Briefly, cells were pre-treated with RRP aqueous extract at concentrations of 50, 100, and 150 $\mu g \cdot mL^{-1}$ for 1 h, followed by stimulation with erastin for 24 h. After treatment, the cells were collected and washed with sterile PBS. FITC-labeled AV was used as a probe in conjunction with PI. The AV/PI signals were detected using a CytoFLEX flow cytometer (Beckman Coulter, Pasadena, CA) to determine the extent of apoptosis.

Western blotting analysis

Western blotting analysis was conducted as previously described [21]. Briefly, proteins from cells and liver tissues were lysed using RIPA buffer (BIORIGIN). The lysed proteins were separated by SDS-PAGE and then transferred onto a polyvinylidene fluoride (PVDF) membrane (Merck Millipore, Darmstadt, Germany). The membranes were incubated overnight at 4 °C with primary antibodies against ZIP14, transferrin, and hepcidin. Following the primary antibody incubation, the membranes were incubated with the appropriate secondary antibodies for 1 h. The protein bands were then visualized using the ChemiDoc™ Touch Imaging System (Bio-Rad, Hercules, CA).

Immunofluorescence

Cellular production of ROS was assessed using the ROS assay kit (S0033, Beyotime Biotechnology, Shanghai, China) according to the manufacturer's instructions [22]. Briefly, cells were pre-treated with RRP aqueous extract at concentrations of 50, 100, and 150 μg·mL^{-1} for 1 h, followed by treatment with MCT or erastin for 24 h. Subsequently, the cells were stained with 10 μmol·L^{-1} DCFH-DA at 37 °C for 20 min. After washing with sterile PBS and staining with DAPI, the cells were imaged using an Olympus FV3000 confocal laser scanning microscope (Tokyo, Japan).

TUNEL assay

The terminal deoxynucleotidyl transferase dUTP nick end labeling (TUNEL) assay was conducted on liver tissues and BRL cells using the TUNEL assay kit (C1089, Jiangsu Institute of Biotechnology, China) according to the manufacturer's protocol [23]. Briefly, BRL cells were fixed with 4% paraformaldehyde for 30 minutes and then permeabilized with 0.1% Triton X-100 for 10 min. The cells were treated with the TUNEL reaction mixture for 1 h in the dark at room temperature. The percentage of TUNEL-positive cells and the number of apoptotic cells in liver tissues and hepatocytes were quantified using an Olympus FV3000 confocal laser scanning microscope (Tokyo, Japan).

Statistical analysis

All experiments were repeated independently at least three times, and the results are presented as mean ± SD. Data were analyzed using one-way ANOVA followed by Tukey's post hoc test for multiple group comparisons, using GraphPad Prism Software 8.0 (GraphPad, San Diego, CA, USA). A P value of ≤ 0.05 was considered statistically significant.

Results

Chemical characterization of RRP

High-performance liquid chromatography (HPLC) was employed to characterize the chemical composition of RRP aqueous extract, owing to its advantages in specificity, sensitivity, and analytical efficiency. An HPLC method was developed to verify the composition and quality of the RRP extract. By using solvents with different polarities, three primary chemical components of RRP—acteoside, rehmannioside D, and 5-hydroxymethylfurfural—were separated and identified. The retention times for these components and mixed standards were determined (Fig. S1A), demonstrating excellent separation and repeatability. Upon analyzing the RRP aqueous extract, the retention times for acteoside, rehmannioside D, and 5-hydroxymethylfurfural were found to be 61, 62, and 8 min, respectively (Fig. S1B).

RRP aqueous extract ameliorates ischemia reperfusion-induced liver injury in mice

To investigate the therapeutic potential of RRP aqueous extract in HIRI, we administered varying dosages of RRP aqueous extract (2.5, 5, and 10 g·kg^{-1}) or a vehicle control to mice subjected to HIRI, as detailed in the "**Materials and methods**" section (Fig. 1A). As shown in Fig. 1B, treatment with RRP aqueous extract significantly restored the organ coefficient and reduced hepatic edema compared to the model group. Moreover, RRP aqueous extract reduced serum levels of ALT and AST, key biomarkers of liver injury. It also ameliorated hepatic oxidative stress by decreasing LDH activity and enhancing NO expression (Fig. 1C). Histopathological analysis with H&E staining (Fig. 1D and Fig. S2A) revealed that the HIRI group displayed disrupted hepatic lobular structures, hemorrhagic foci, and hepatocyte necrosis. In contrast, medium and high dosages of RRP aqueous extract significantly improved hepatic morphology, including the integrity of liver cell nuclei and lobules. TUNEL staining was used to evaluate apoptosis in liver tissues. The number of apoptotic cells was markedly lower in the livers of mice treated with RRP aqueous extract compared to the HIRI group (Fig. 1E and Fig. S2B). Considering the role of inflammation in HIRI, we assessed the expression of several inflammatory markers. qPCR analysis indicated elevated levels of inflammatory cytokines *il-6*, *il-1*, and and the M1 macrophage marker inducible nitric oxide synthase (*inos*) in the HIRI group. These levels were significantly reduced following RRP aqueous extract treatment. Additionally, the mRNA expression of endothelial nitric oxide synthase (*enos*), an enzyme that produces NO and exerts vasoprotective effects, was decreased after HIRI surgery but was restored by RRP aqueous extract administration (Fig. 1F). These findings suggest that RRP aqueous extract effectively mitigates hepatic inflammation and liver damage induced by HIRI surgery.

RRP aqueous extract influences the differential expression of ferroptosis-associated genes in mice

To investigate the therapeutic role of RRP aqueous extract in HIRI, we conducted RNA-sequencing analysis on liver tissues from HIRI mice treated with RRP aqueous extract. Volcano plots revealed DEGs between the sham and HIRI groups, as well as between the HIRI and HIRI + RRP groups ($\log_2$ fold change C > 0.20. adjusted P-value < 0.05). Among these DEGs, ferroptosis-related genes *hspb1* and *slc7a11* were significantly upregulated, while *slc39a14* and *hamp* were significantly downregulated following RRP aqueous extract treatment (Fig. 2A). We annotated these DEGs and performed KEGG pathway analysis, which showed that genes in the HIRI group were significantly enriched in processes such as apoptosis, immune regulation, and endoplasmic reticulum stress. In contrast, genes in the HIRI + RRP group were enriched in pathways related to mitochondrial energy metabolism, cell cycle regulation, and nucleic acid metabolism. Notably, the ferroptosis pathway was significantly enriched after RRP aqueous extract administration (Fig. 2B). Gene Ontology (GO) analysis corroborated these findings, indicating that DEGs in the HIRI group were primarily involved in cell growth and death, material and energy metabolism, signal transduction, and interaction processes. In comparison, DE-

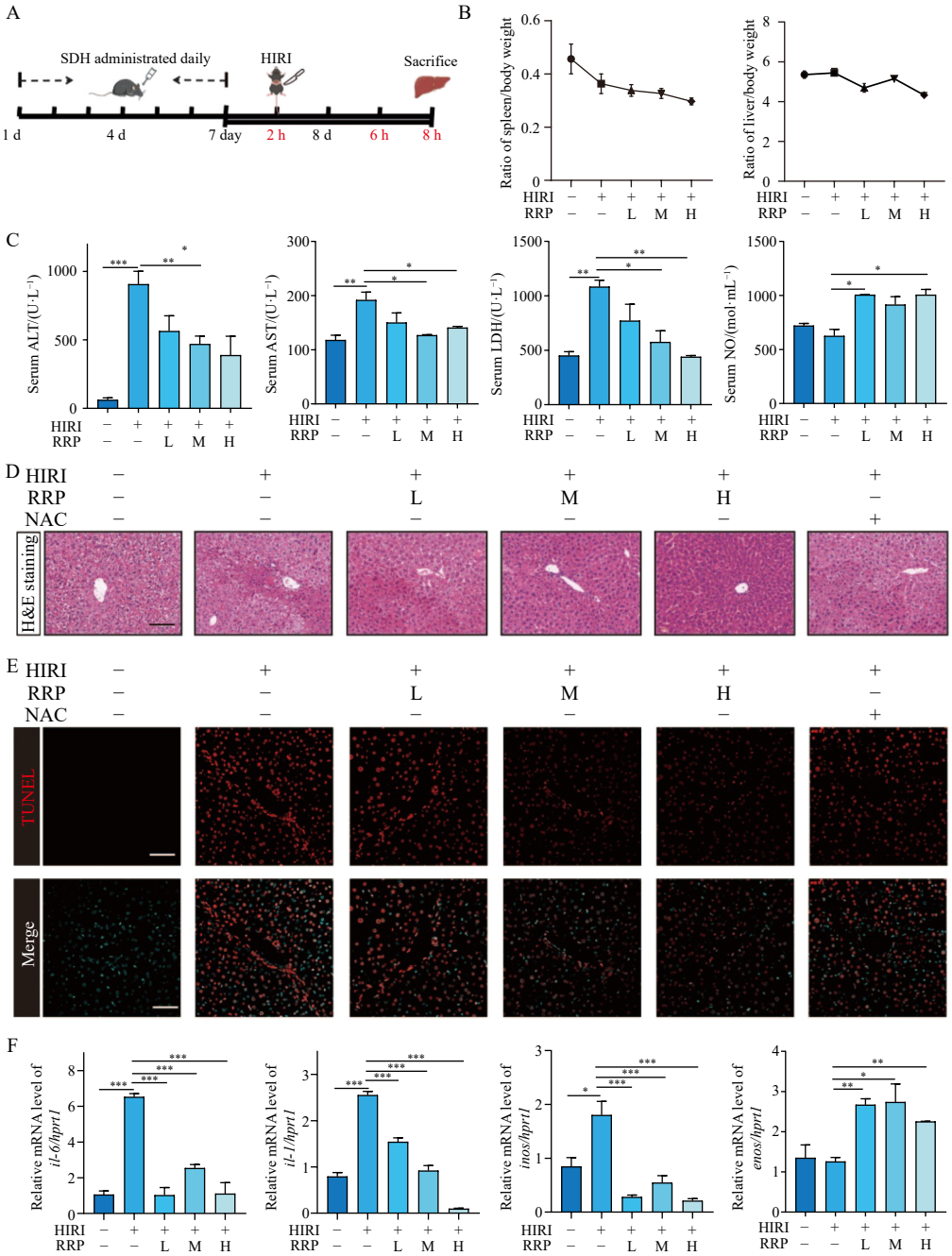

Fig. 1 Effects of RRP aqueous extract on HIRI mice. A surgical model of HIRI was established and treated with different doses of RRP aqueous extracts for one week, as indicated. (A) Flow chart of animal experiments. (B) Measurement of spleen/body weight ratio and liver/body weight ratio after sham surgery or HIRI. (C) Serum ALT, AST, LDH and NO levels. (D) Representative images of H&E staining were quantified using Image J software. Scale bar = 100 μm. (E) TUNEL staining images of livers. Scale bar = 50 μm. (F) Relative mRNA levels of *il-6*, *il-1*, *inos*, and *enos* in liver tissues were determined by qPCR and normalized using *hprt1* as an internal control. Statistical significance: $^{*}P < 0.05$, $^{**}P < 0.01$, $^{***}P < 0.001$ ($n = 6$).

Gs in the HIRI + RRP group were mainly associated with energy metabolism, redox responses, immune responses, gene expression, and cell cycle processes (Fig. 2C). Gene Set Enrichment Analysis (GSEA) further supported these observations (Fig. 2D). Post-ischemia-reperfusion surgery, genes related to the cell cycle and apoptosis were highly expressed in the HIRI group. After RRP aqueous extract treatment, genes involved in ferroptosis were significantly enriched. These results suggest that RRP aqueous extract exerts its therapeutic effects on HIRI by modulating ferroptosis-related processes and improving iron metabolism homeostasis in mice.

RRP aqueous extract reduces ferroptosis and improves mitochondria structure in HIRI-induced mice

While our previous findings demonstrated that RRP aqueous extracts improved HIRI and may influence mitochondrial energy and ferroptosis-related processes, detailed

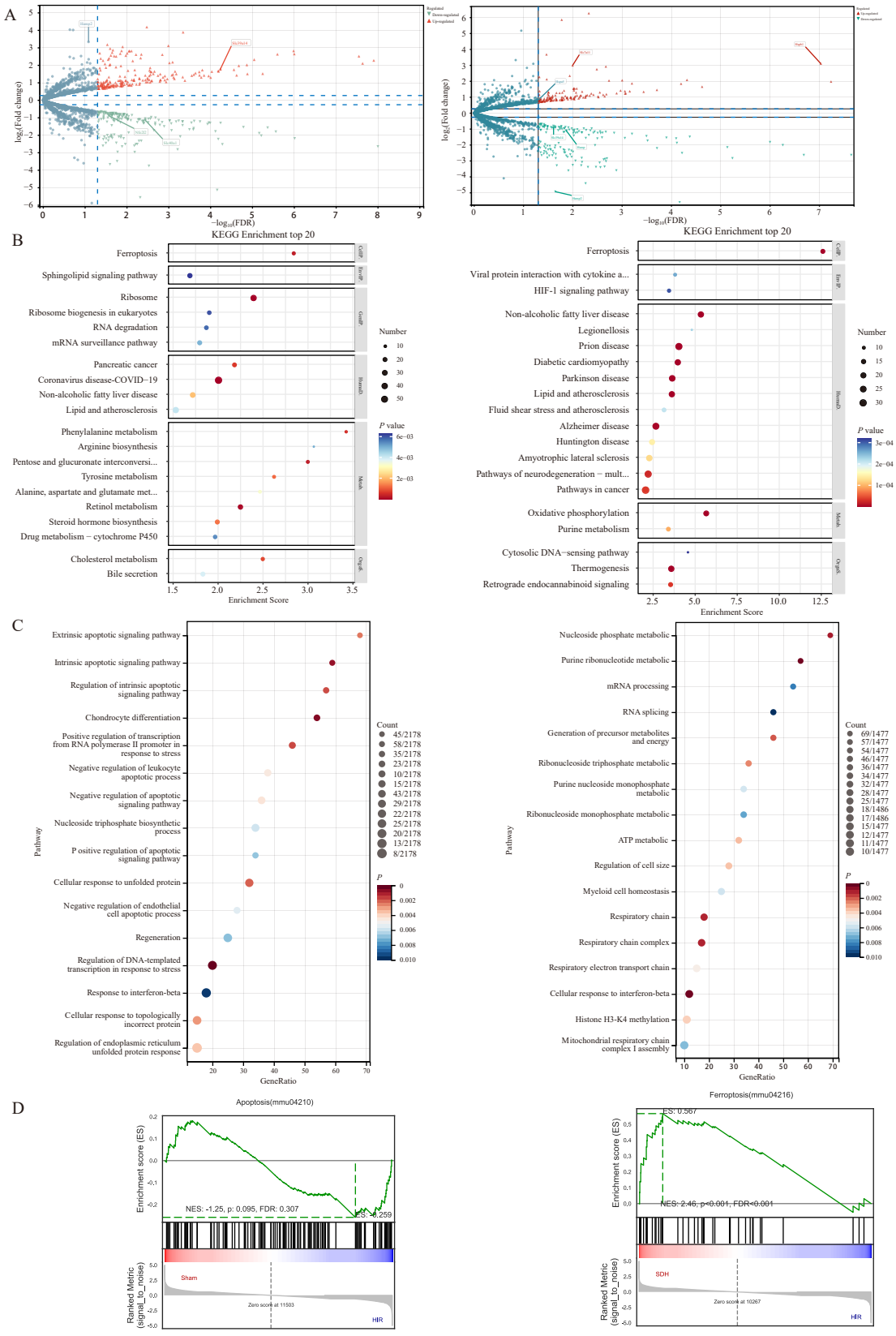

Fig. 2 Transcriptomic analysis of RRP aqueous extract-treated livers. (A) Volcano plots of DEG expression in liver samples, (B) KEGG pathway, (C) GO enrichment circle diagram, and (D) GSEA analysis from sham and HIRI groups (left panel), and HIRI and HIRI + RRP groups (right panel).

experimental evidence on how RRP relieves ferroptosis to alleviate liver IRI was still lacking. To address this, we performed heatmap cluster analysis on differentially expressed genes (DEGs) related to ferroptosis. The left panel of Fig. 3A shows that RRP aqueous extract increased the expression of genes associated with mitochondrial energy metabolism and redox response, such as *noa1* (nitric oxide associated 1), *cyp2c70* (cytochrome P450, family 2, subfamily c, poly-

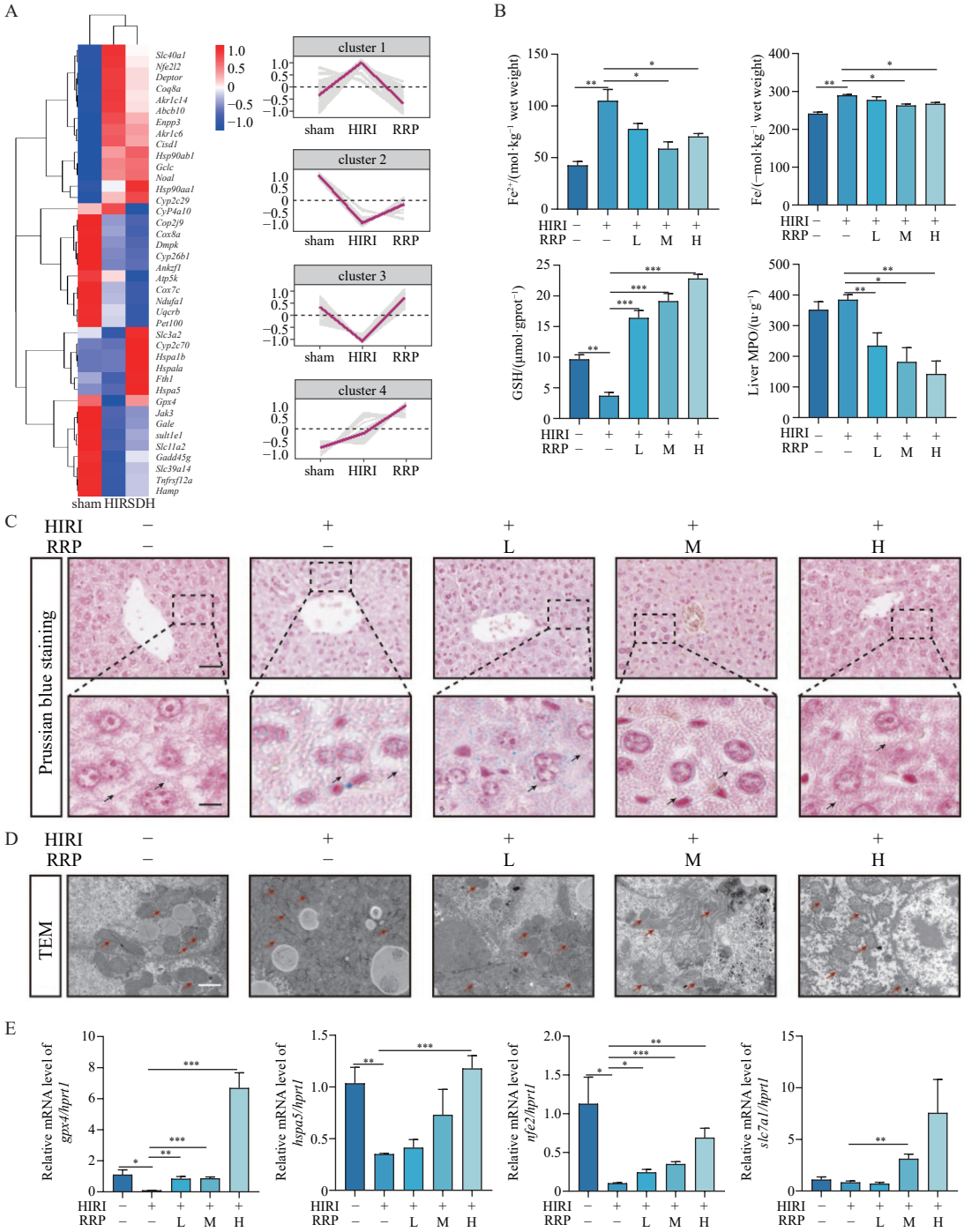

Fig. 3 RRP aqueous extract attenuates ferroptosis in the liver with HIRI. (A) The relative expression levels of DEGs associated with ferroptosis were shown in the heat map. The right panel divides the expression of DEGs into four categories and plots trend lines reflecting the hepatic changes in these DEGs. (B) Ferrous ion, total iron ion, GSH, and MPO contents in the mouse liver. (C) Prussian staining of the liver in each group of mice. Scale bar = 60 μm. (D) Representative transmission electron microscopy images of mitochondria in hepatocytes of the liver. Red arrow: damaged mitochondria. Scale bar = 1 μm. (E) Relative mRNA expressions of *gpx4*, *hspa5*, *nfe2l2*, and *slc7a11* in each group were determined by qPCR and normalized using *hprt1* as an internal control. Statistical significance: $^{*}P < 0.05$, $^{**}P < 0.01$, $^{***}P < 0.001$ ($n = 6$).

peptide 70). Conversely, it downregulated genes linked to iron metabolism, such as *hamp* and *slc39a14*, in response to HIRI. The right panel of Fig. 3A categorizes these DEGs into four clusters, displaying trend lines that reflect these hepatic changes. Pretreatment with RRP aqueous extract significantly reduced the accumulation of intrahepatic ferrous and total iron ions induced by HIRI, thereby suppressing intrahepatic ferroptosis (Fig. 3B). The levels of GSH, the most abundant intracellular antioxidant responsible for scavenging ROS catalyzed by GPX4, markedly increased after RRP aqueous extract pretreatment, indicating reduced ROS accumulation in the liver. Additionally, myeloperoxidase (MPO), a marker of neutrophil activation, was significantly reduced by RRP aqueous extract pretreatment, contributing to decreased hepatic inflammation (Fig. 3B). RRP also mitigated oxidative stress-induced liver damage, as evidenced by increased superoxide dismutase (SOD) and NO levels, along with a significant reduction in MDA, a marker of lipid peroxidation (Fig. S3A). Considering the Fenton reaction's conversion mechanism between trivalent and divalent iron ions, we discovered that trivalent iron ions were also downregulated following RRP aqueous extract pretreatment. Fig. 3C shows significant intracellular iron ion accumulation in the HIRI group (indicated by higher Prussian blue staining), which was significantly ameliorated by RRP aqueous extract in a dose-dependent manner. TEM results in Fig. 3D further confirmed that mitochondrial membranes were damaged and cristae were reduced or absent in the HIRI group, while the mitochondrial structure was significantly preserved with RRP treatment. As indicated in Fig. 3E, the hepatic expression of genes responsible for preventing ferroptosis, such as *gpx4*, *hspa5* (heat shock protein family A member 5), *nfe2l2* (NFE2 like bZIP transcription factor 2), and *slc7a11*, was substantially decreased following HIRI but was remarkably restored by RRP aqueous extract treatment (Fig. 3E).

RRP aqueous extract attenuates ferroptosis in hepatocytes after MCT or erastin intervention

While previous data demonstrated that RRP aqueous extract alleviates ferroptosis *in vivo* in cases of hepatic ischemia-reperfusion injury (HIRI), its effects *in vitro* remained unclear. To address this, we selected the top 1205 genes significantly affected in our RNA-sequencing data of whole livers. We discovered that most of these genes were enriched in hepatocytes (Fig. 4A). Consequently, we focused on investigating the role of RRP aqueous extract on hepatocytes treated with MCT or the ferroptosis inducer erastin. Initially, a CCK8 assay was used to determine the optimal concentration of RRP aqueous extract by assessing cell growth and proliferation, confirming doses of 50, 100, and 150 μg·mL^{-1} for RRP aqueous extract administration (Fig. S4A). PCR results indicated that genes inhibiting ferroptosis, such as *gpx4*, showed an upward trend following RRP administration. In contrast, the intracellular ferroptosis marker prostaglandin-endoperoxide synthase 2 (*ptgs2*) exhibited a decreasing trend after pretreatment with RRP aqueous extract (Fig. 4B). As shown in Fig. S4B, similarly, *slc7a11* expression increased in both MCT- and erastin-treated groups after RRP administration. Additionally, mRNA levels of *p53*—which promotes ferritin formation —and the inflammatory factor *il-6* increased after MCT or erastin stimulation but decreased following RRP administration. Flow cytometry was employed to verify whether RRP aqueous extract could mitigate ferroptos-

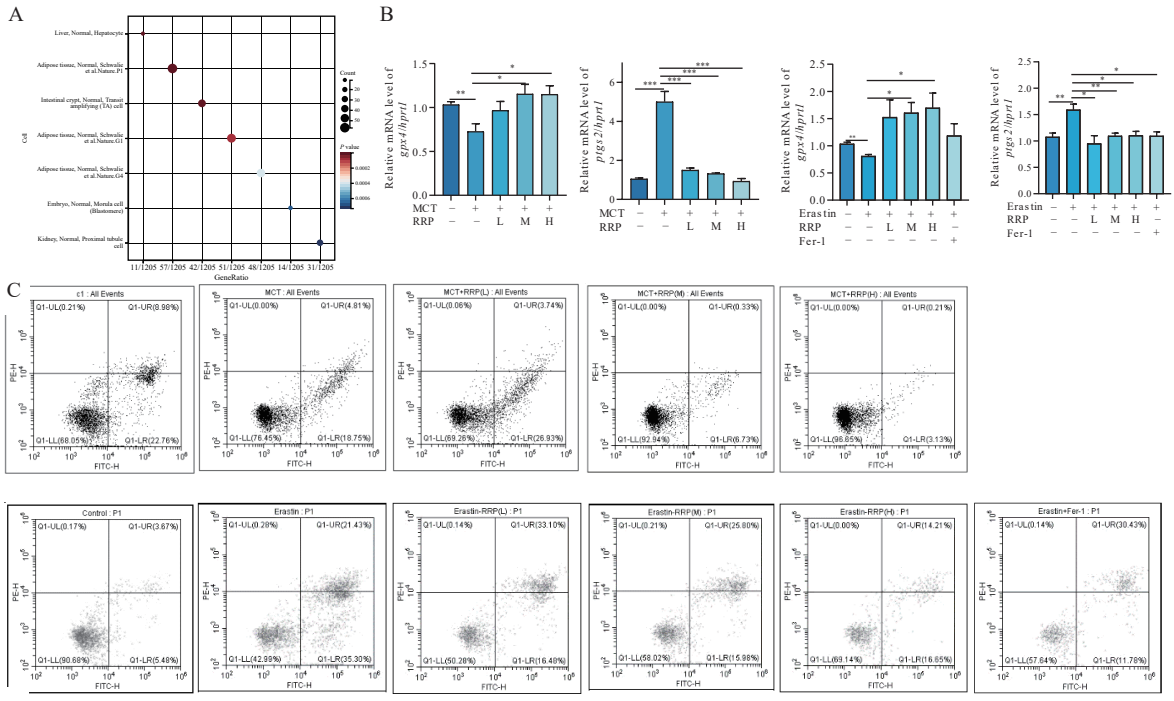

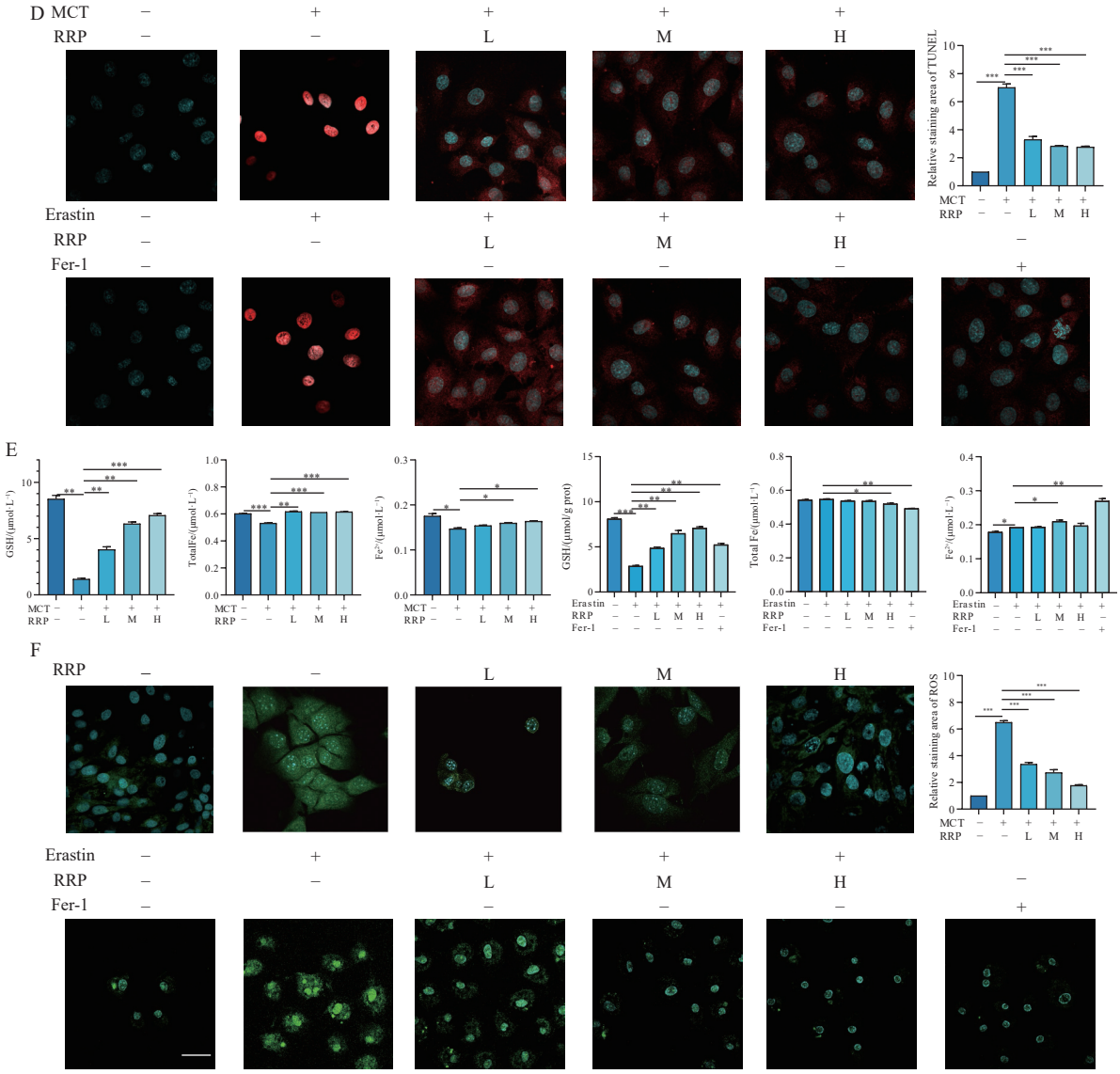

Fig. 4 RRP aqueous extract attenuates ferroptosis in injured hepatocytes. (A) Cell sorting enrichment. (B) Relative mRNA expressions of *gpx4* and *ptgs2* in each group were determined by qPCR and normalized using *hprt1* as an internal control. (C) Flow cytometry of AV-PI with histograms. (D) TUNEL staining of hepatocytes. Scale bar = 30 μm. (E) GSH, total iron ion and ferrous ion contents in hepatocytes. (F) Representative images of live cell staining of ROS. Scale bar = 30 μm. Statistical significance: $^{*}P < 0.05$, $^{**}P < 0.01$, $^{***}P < 0.001$ ($n = 3$).

is (Fig. 4C and Fig. S4C). Both MCT and erastin significantly increased the number of early apoptotic hepatocytes, but RRP aqueous extract effectively blocked this process. TUNEL staining further confirmed these results, showing that pretreatment with RRP aqueous extract significantly reduced hepatocyte apoptosis induced by MCT or erastin (Fig. 4D and Fig. S4D). Given that increased iron absorption or limited iron efflux can lead to iron buildup and subsequent ferroptosis *via* various signaling pathways [24], we investigated the relationship between RRP aqueous extract-mediated hepatoprotection and iron buildup. RRP aqueous extract effectively increased GSH levels and reduced intracellular iron uptake, as evidenced by decreased total and ferrous iron ion levels in the cell medium, thereby mitigating MCT or erastin-stimulated ferroptosis (Fig. 4E). These findings suggest that RRP aqueous extract influences the ferroptosis network by modulating iron ion endocytosis and efflux. Ferroptosis is also known as a ROS-dependent form of cell death, making ROS a critical feature of ferroptosis. To detect cellular ROS generation (green fluorescence), we employed live cell staining techniques in Fig. 4F and Fig. S4E. RRP aqueous extract significantly reduced ROS levels induced by MCT or erastin in hepatocytes. Overall, these findings suggest that RRP aqueous extract acts as a potential natural agent exerting hepatoprotective effects in HIRI by inhibiting ferroptosis.

RRP aqueous extract attenuates ferroptosis both in vivo and in vitro via regulating intracellular iron homeostasis

After initially confirming that RRP aqueous extract can

alleviate HIRI by suppressing ferroptosis, we aimed to further explore its role in mitigating iron toxicity. We generated a genetic heatmap to identify ferroptosis-associated genes affected by RRP aqueous extract pretreatment (Fig. 5A). Western blotting analysis showed that RRP aqueous extract dose-dependently reduced the levels of transferrin, ZIP14, and hepcidin induced by HIRI (Fig. 5B). To validate these findings, qPCR experiments were conducted. The results showed that genes involved in iron metabolisms, such as *hamp*, *slc39a14*, and *fth1* (ferritin heavy polypeptide 1), which regulate iron endocytosis and efflux, were downregulated after administration of RRP aqueous extract. Conversely, genes such as *cisd1* and *slc40a1*, which inhibit ferric ion uptake and promote mitochondrial iron utilization, were upregulated following RRP pretreatment (Fig. 5C). Additionally, inflammatory markers such as *il-6* and *il-1* were significantly downregulated after RRP aqueous extract administration, while *hspb1* and *slc11a2*, which inhibit ROS synthesis, were significantly upregulated, synergistically contributing to hepatoprotective effects (Fig. S5A). We also examined the nuclear translocation of hepcidin in hepatocytes labeled with HNF4α. Immunofluorescence co-staining showed that the increased nuclear expression of hepcidin caused by HIRI was significantly and dose-dependently reduced by RRP aqueous extract (Fig. 5D and Fig. S5B). Moreover, the expression of the transmembrane protein ZIP14, which transports extracellular iron into cells, was significantly increased in the HIRI group but rapidly decreased with increasing doses of RRP aqueous extract (Fig. 5E and Fig. S5C).

RRP aqueous extract attenuates ferroptosis in vitro by regulating intracellular iron homeostasis

Building on our previous observations, we further investigated the role of RRP aqueous extract in mitigating ferroptosis induced by HIRI *in vitro* cell models. As illustrated in Fig. 6A, genes that promote ferroptosis, such as *hamp*, *slc39a14*, and *fth1*, were significantly downregulated under both MCT and erastin treatments following pre-administration of RRP aqueous extract. Conversely, genes that inhibit ferroptosis, including *cisd1* and *slc40a1*, were significantly upregulated after RRP aqueous extract administration (Fig. 6B). Moreover, pretreatment with RRP aqueous extract led to a significant upregulation of *hspb1* in both models, indicating inhibition of transferrin receptor protein 1 (TFRC) and a reduction in intracellular ROS production (Fig. S6A). Western blotting analysis further confirmed the protective role of RRP aqueous extracts in reducing ferroptosis during HIRI, as shown by decreased levels of ZIP14 and hepcidin (Fig. 6C). As shown in Fig. 6D and Fig. S6B, Fluorescence staining of hepcidin (red fluorescent area) corroborated our *in vivo* findings, showing a significant reduction in nuclear hepcidin expression with increasing doses of RRP aqueous extract. Additionally, ZIP14 expression in hepatocyte membranes significantly decreased with increasing doses of RRP aqueous extract following MCT or erastin induction (Fig. 6E and Fig. S6C). These findings suggest that RRP aqueous extract effectively mitigates intracellular ferroptosis by regulating the expression of hepcidin and ZIP14 *in vivo* and *in vitro*.

Inhibition of hamp ameliorates ferroptosis and enhances the protective effect of RRP aqueous extract against HIRI

Our results indicated that *hamp*, a central component of the *hamp/slc40a1/slc39a14* regulatory loop, plays a crucial role in the amelioration of HIRI by RRP aqueous extracts. To further investigate this, we used siRNA to determine whether inhibiting *hamp* could synergistically enhance the protective effect of RRP aqueous extracts. Three siRNAs targeting *hamp* were designed, and siRNA1 was selected for subsequent experiments (Fig. 7A). Downregulation of *hamp* significantly alleviated ferroptosis by promoting intracellular ferrous ion efflux. Furthermore, RRP aqueous extract synergistically corrected the HIRI-induced imbalance in intracellular iron homeostasis (Fig. 7B). Compared with the control group, *hamp* inhibition resulted in higher levels of GSH and NO, which were further enhanced by RRP aqueous extract. Additionally, MDA levels were significantly decreased, and SOD levels were significantly increased after *hamp* inhibition and RRP aqueous extract treatment (Fig. 7C). As shown in Fig. 7D, ROS staining revealed that *hamp* inhibition, combined with RRP aqueous extract, significantly reduced ROS accumulation caused by ferroptosis. Following erastin induction, the expression of hepcidin and ZIP14 was significantly suppressed in the si-*hamp* group compared to the erastin group. This inhibition was even more pronounced in the group treated with both RRP aqueous extract and si-*hamp* (Figs. 7E and 7F). In conclusion, inhibiting *hamp* synergizes with RRP aqueous extract to reduce lipid peroxidation and ameliorate HIRI-induced ferroptosis, highlighting a potential therapeutic strategy for liver injury.

Discussion

RRP is an herbal remedy that contains numerous active ingredients, offering synergistic therapeutic benefits by targeting multiple pathways simultaneously. In this study, we confirmed the anti-ferroptosis efficacy of RRP aqueous extract in a HIRI-induced mouse model and in MCT- and erastin-stimulated hepatocytes. Through HPLC, RNA-sequencing analysis, and molecular biology experiments, we demonstrated that RRP aqueous extract effectively mitigates HIRI-induced liver injury, inflammation, and mitochondrial damage in mouse livers. Additionally, it improved apoptosis, reduced intracellular ROS levels, and decreased ferrous ion accumulation in MCT- or erastin-stimulated hepatocytes. Significantly, we found that the hepatoprotective effects of RRP aqueous extract, particularly its inhibition of lipid peroxidation and cell apoptosis in hepatocytes under hypoxic-ischemic conditions, are largely dependent on the regulation of iron metabolism. This includes decreasing *hamp* expression, promoting FPN-mediated transport of ferrous ions to the extracellular space, reducing ZIP14 expression to inhibit the import of extracellular iron ions, increasing *cisd1* expression to enhance intracellular iron ion utilization, and upregulating

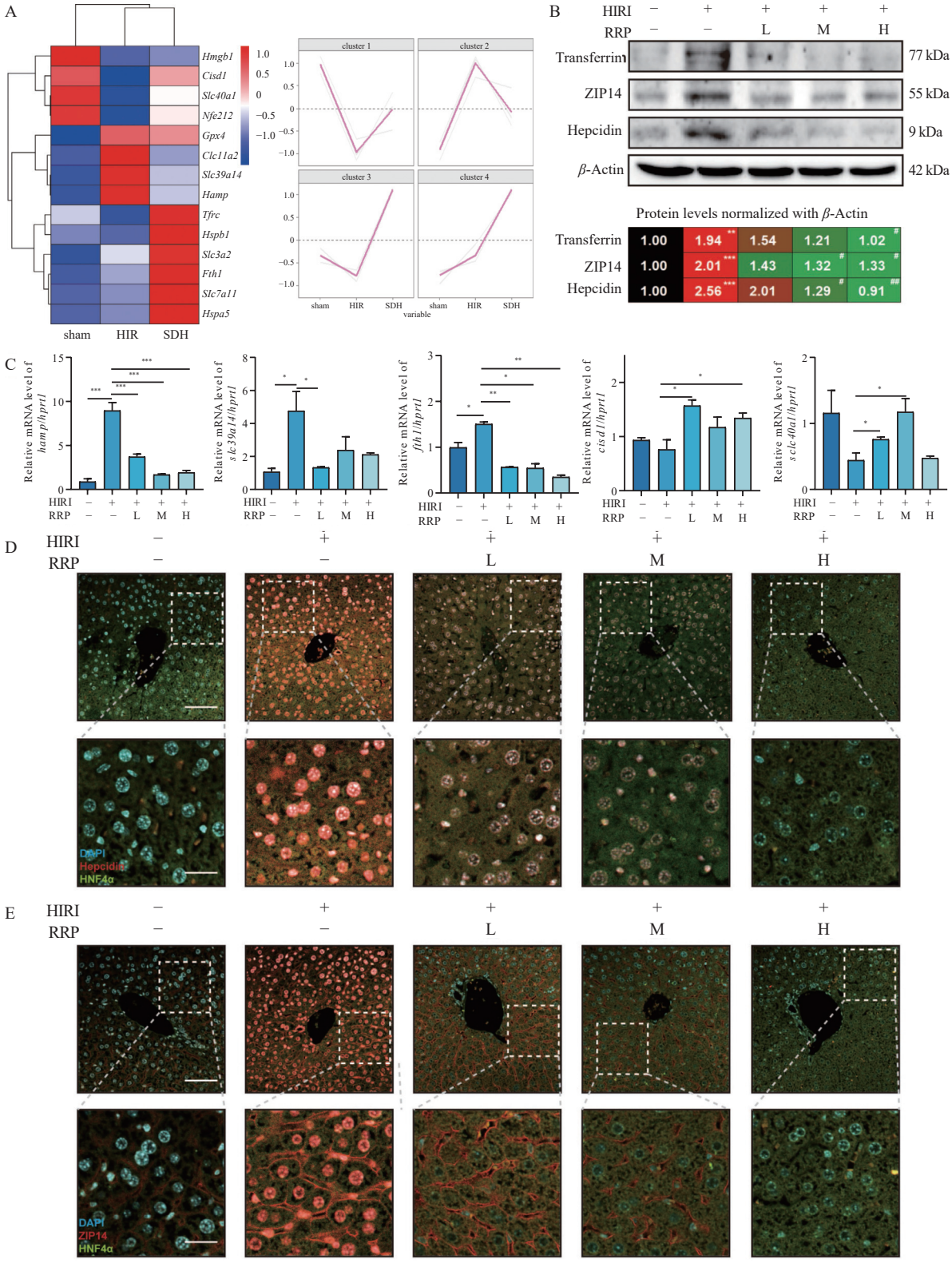

Fig. 5 RRP aqueous extract alleviates ferroptosis *via* improving intracellular iron homeostasis. (A) A heat map with ferroptosis-related genes. (B) The protein expressions of transferrin, ZIP14, and hepcidin in the liver and normalized with *β*-actin. (C) Relative mRNA expressions of *hamp*, *slc39a1*, *fth1*, *cisd1*, and *slc40a1* in the liver and normalized using *hprt1* as an internal control. Represent immunofluorescence images of (D) HNF4*α* and hepcidin and (E) HNF4*α* and ZIP14 in liver. Scale bar = 100 μm. Statistical significance: $^{*}P < 0.05$, $^{**}P < 0.01$, $^{***}P < 0.001$ ($n = 6$).

hspb1 to mitigate ROS accumulation. Moreover, we identified that the HIRI-induced imbalance of intracellular iron homeostasis is linked to *hamp*, which can be induced by inflammatory factors to produce hepcidin, subsequently inhibiting FPN on the cell membrane and restricting the release of intracellular ferrous ions. Inhibition of *hamp* using specific siRNA further enhanced the inhibitory effect of RRP aqueous extract on ferroptosis. In summary, our findings confirm that RRP aqueous extract provides protection against HIRI by correcting intracellular iron homeostasis and thereby reducing ferroptosis.

Both clinical observations and experimental research have highlighted that the primary and inevitable consequence of HIRI is the death of hepatocytes, the most abundant parenchymal cells in the liver. Ferroptosis is widely recognized as a critical factor in cell death associated with IRI, particularly in acute heart, brain, and kidney injuries [25-27]. The main characteristics of ferroptosis are intracellular iron ion accumulation and lipid peroxidation [28]. Despite the liver being the largest metabolic organ, the mechanisms underlying ferroptosis in HIRI have not been extensively studied. Recent clinical research has shown elevated serum ferritin levels in patients undergoing LT, suggesting that intracellular iron accumulation in the liver significantly contributes to HIRI post-LT [29]. While mechanistic studies of ferroptosis have traditionally focused on the cysteine/GSH/GPX4 antioxidant axis, new evidence is increasingly highlighting the roles of other proteins involved in ferroptosis during HIRI. For instance, hepcidin regulates FPN to control intra- and extracellular iron flow, playing a crucial role in iron metabolism and HIRI progression [30, 31]. Additionally, ZIP14 has been shown to prevent NTBI accumulation and ferroptosis in hepatocytes under conditions of iron overload [32]. Therefore, targeting iron metabolism may offer a promising approach for treating HIRI. Understanding the molecular regulatory mechanisms involved in this process could provide new strategies for the prevention and treatment of diseases related to iron metabolism disorders.

RRP aqueous extract is a traditional herbal remedy known for its beneficial effects on liver function, particularly through its anti-inflammatory and cell proliferation properties [33]. Its active components provide hepatoprotective benefits *via* antioxidant and anti-inflammatory mechanisms [34]. Although RRP aqueous extracts have not been explicitly shown to alter the process of intracellular ferroptosis, they have demonstrated the ability to prevent inflammatory responses and reduce oxidative stress levels in mice [35]. Key components isolated from Radix Rehmanniae, such as epigallocatechin gallate (EGCG), have shown significant hepatoprotective effects. EGCG administration has been found to reduce MDA levels, increase GSH and SOD content, and enhance hepatic antioxidant activity in damaged liver tissues [36]. Additionally, EGCG reduces iron ion levels in liver cells and tissues and provides hepatoprotective effects by suppressing inflammation and protecting mitochondria [37]. These findings suggest that RRP extracts have considerable

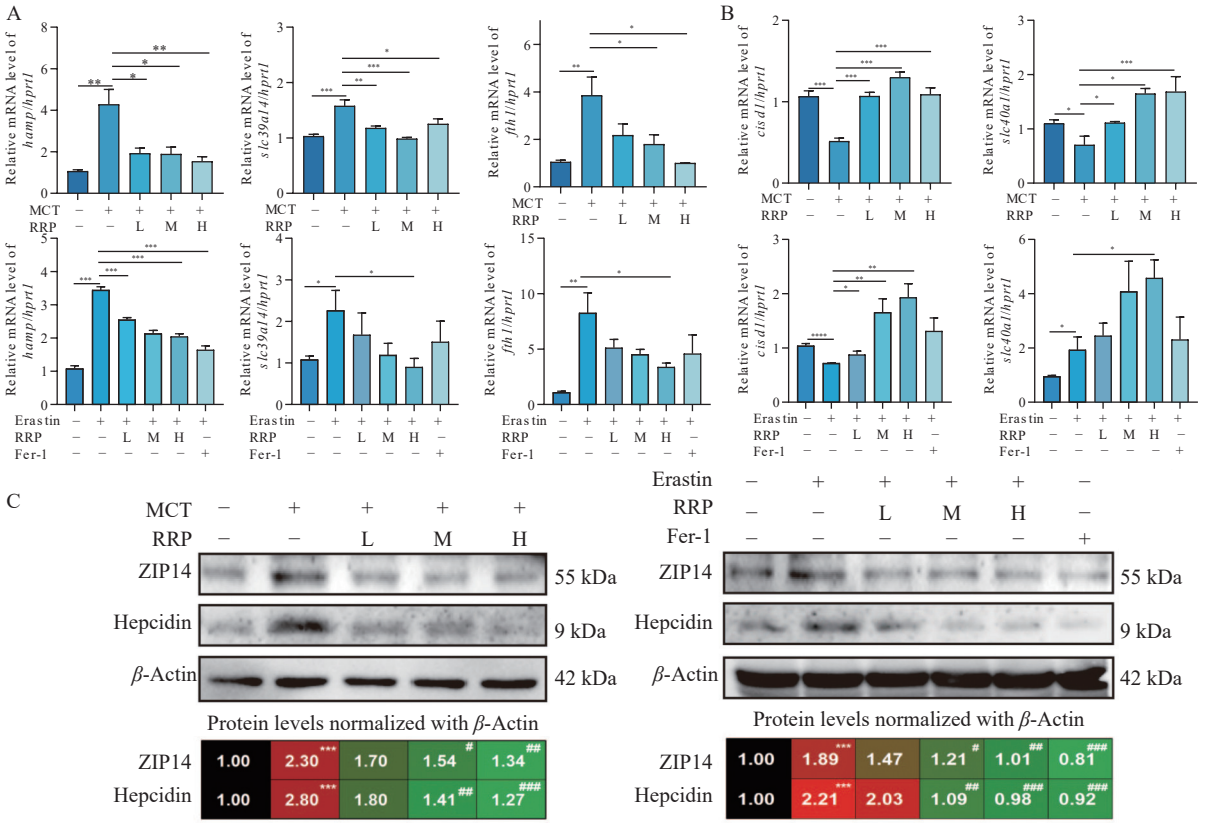

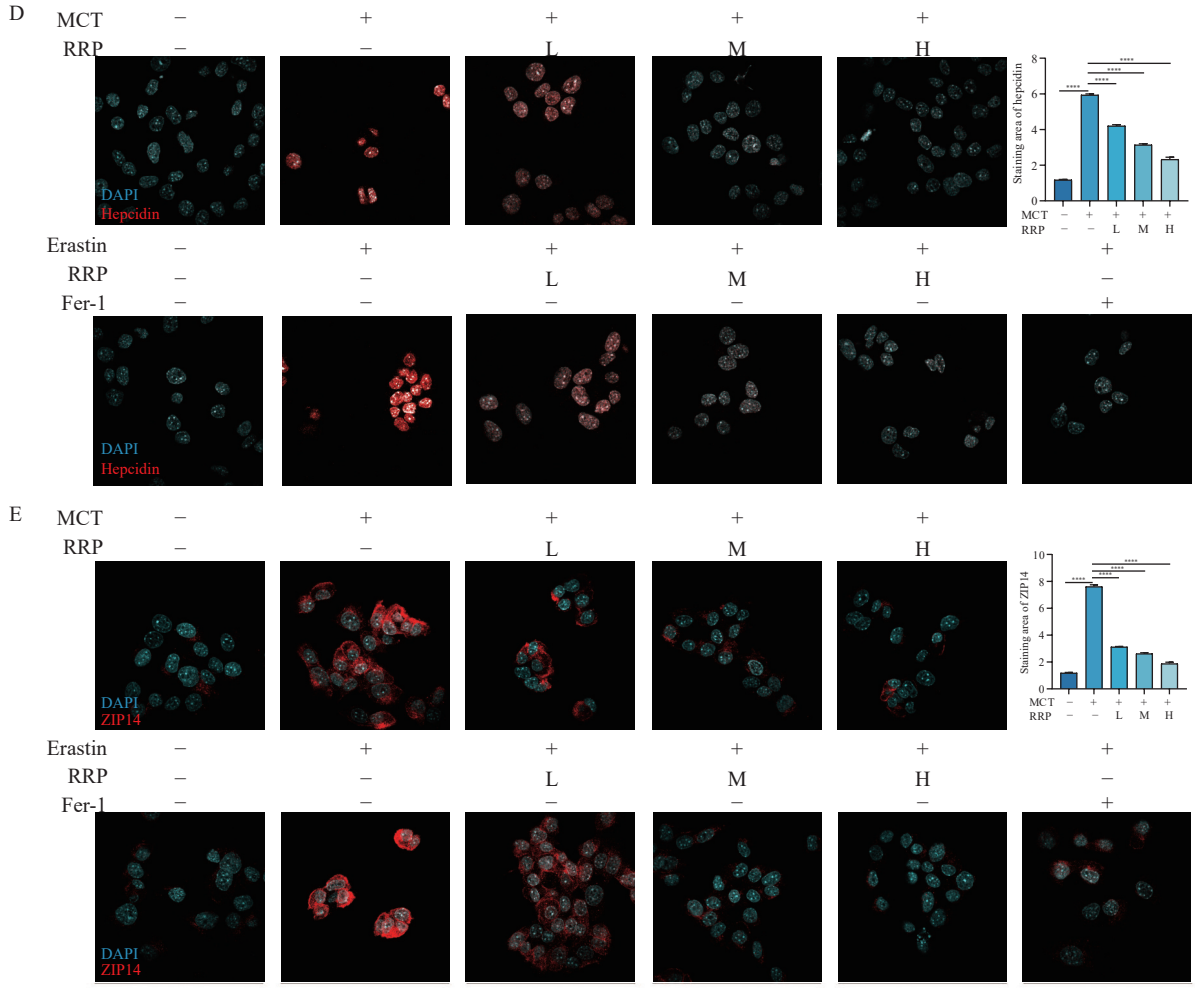

Fig. 6 RRP aqueous extract improves HIRI by regulating ferroptosis *via* improving hepcidin and ZIP14-dominated iron homeostatic network. (A) Relative mRNA expressions of *hamp*, *slc39a14*, and *fth1* in each group were determined by qPCR and normalized using *hprt1* as an internal control. (B) Relative mRNA expressions of *cisd1* and *slc40a1* in each group were determined by qPCR and normalized using *hprt1* as an internal control. (C) The protein expressions of ZIP14 and hepcidin in the cells and normalized with *β*-actin. Represent immunofluorescence images of (D) hepcidin and (E) ZIP14 in hepatocytes. Scale bar = 30 μm. Statistical significance: $^{*}P < 0.05$, $^{**}P < 0.01$, $^{***}P < 0.001$ ($n = 3$).

potential against HIRI. However, the molecular mechanisms linking them to ferroptosis require further investigation. In the current study, we demonstrated that RRP aqueous extract not only reduces inflammation by suppressing the expression of inflammatory markers such as IL-6 and IL-1 but also decreases MDA levels, maintains normal mitochondrial structure and cristae density, and improves lipid peroxidation. Furthermore, we discovered that pretreatment with RRP aqueous extract partially reversed the expression of *hamp*, *zip14*, and *slc11a2* in HIRI-induced liver damage. Despite the decreased intracellular concentrations of total and ferrous iron ions, the iron content in the medium was higher, suggesting that RRP aqueous extract helps cells restore iron transport and storage utilization activities, thereby maintaining iron homeostasis.

This study demonstrates the hepatoprotective effects of RRP aqueous extract against HIRI by modulating intracellular iron homeostasis and reducing ferroptosis. However, several limitations remain that require further investigation. Our results showed consistent changes in the expression of *hspb1*, *slc40a1*, and *cisd1* in both mouse livers and *in vitro* hepatocyte models, while the gene changes of *slc39a14* and hamp were not consistent. We speculate that: 1) *hspb1* is sensitive to real-time ROS production and may block trivalent iron by inhibiting TFRC uptake of iron ions. 2) *slc40a1*, as a key route for divalent iron ion export, plays a crucial role in maintaining intracellular iron homeostasis. 3) *Cisd1* aids in the intracellular buildup of divalent iron ions, facilitating their entry into the mitochondrial TCA cycle and increasing their utilization within the cell. These iron-sensitive genes—*hspb1*, *slc40a1*, and *cisd1*—likely work synergistically to efficiently regulate iron ion absorption, exportation, and utilization. Conversely, *hamp*, activated by extracellular inflammatory stimuli, inhibits FPN and plays a critical role in iron metabolism regulation. The higher *hamp* expression in tissues compared to *in vitro* hepatocytes might be due to a more pro-

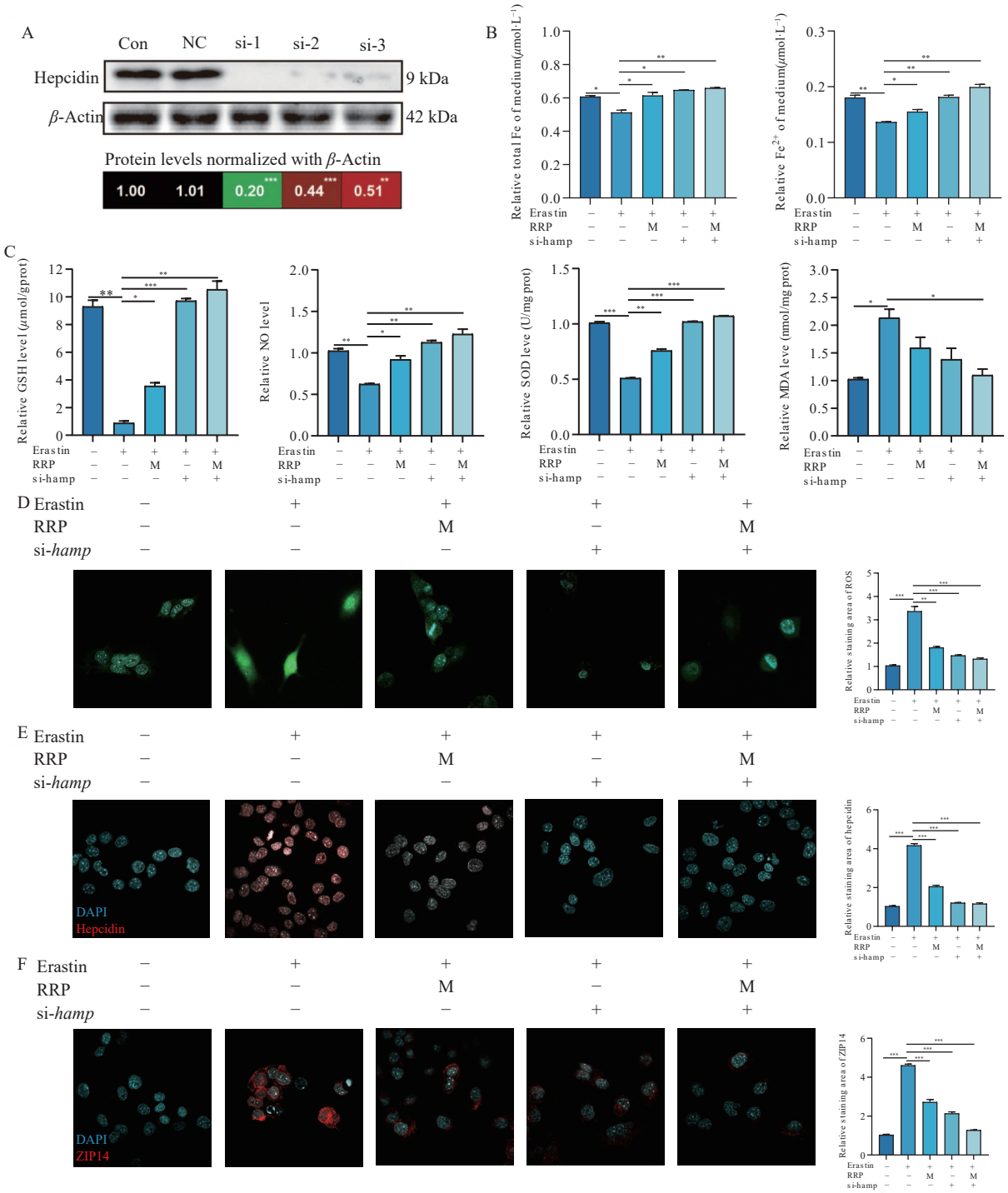

Fig. 7 Inhibition of *hamp* can synergize with RRP aqueous extracts to improve intracellular iron homeostasis and attenuate HIRI. (A) The protein expression of hepcidin in hepatocytes transfected with different *hamp* siRNAs and normalized with *β*-actin. (B) Total ferrous and ferrous ion levels in the culture medium. (C) GSH, NO, MDA, SOD levels in hepatocytes. (D) Representative images of live cell staining of ROS. Represent immunofluorescence images of (E) hepcidin and (F) ZIP14 in cells. Scale bar = 30 μm. Statistical significance: $^{*}P < 0.05$, $^{**}P < 0.01$, $^{***}P < 0.001$ ($n = 3$).

nounced inflammatory environment *in vivo*. Another important consideration is the dual role of *fth1*. While it stores iron ions as a component of ferritin, supporting intracellular iron homeostasis [38], it also facilitates ferritin degradation in lysosomes, releasing free iron and inducing ferroptosis [39]. Our findings show that RRP can inhibit *fth1* mRNA levels in both liver tissues and hepatocytes. We propose that RRP aqueous extract reduces the potential of *fth1* to enhance iron release from ferritin by increasing iron autophagy, thus mitigating ferroptosis. Despite demonstrating the hepatoprotective ef-

fects of RRP against HIRI by restoring intracellular iron homeostasis, further studies are urgently needed. Specifically, research should focus on identifying which components of RRP aqueous extracts affect specific aspects of ferroptosis in hepatocytes. This knowledge is crucial for translating our findings into clinical applications and developing targeted therapies for liver injury.

Conclusion

This study shows that RRP aqueous extract attenuates HIRI-induced liver damage, inflammation, and ferroptosis by inhibiting iron uptake and promoting iron excretion, thereby maintaining intracellular iron homeostasis. We explored the underlying molecular mechanisms in both *in vivo* and *in vitro* models. Our findings provide direct experimental evidence of the hepatoprotective effects of RRP on HIRI and suggest a novel therapeutic strategy for clinical application in HIRI patients.

Supporting Information

Supporting information can be requested by sending E-mail to the corresponding author.

References

[1] Nastos C, Kalimeris K, Papoutsidakis N, *et al*. Global consequences of liver ischemia/reperfusion injury [J]. *Oxid Med Cell Longev*, 2014, **2014**: 906965.

[2] Chen SY, Zhang HP, Li J, *et al*. Tripartite motif-containing 27 attenuates liver ischemia/reperfusion injury by suppressing transforming growth factor *β*–activated kinase 1 (TAK1) by TAK1 binding protein 2/3 degradation [J]. *Hepatology*, 2021, **73**(2): 738-758.

[3] Cannistra M, Ruggiero M, Zullo A, *et al*. Hepatic ischemia reperfusion injury: a systematic review of literature and the role of current drugs and biomarkers [J]. *Int J Surg*, 2016, **33**: S57-S70.

[4] Han H, Desert R, Das S, *et al*. Danger signals in liver injury and restoration of homeostasis [J]. *J Hepatol*, 2020, **73**(4): 933-951.

[5] Liu H, Man K. New insights in mechanisms and therapeutics for short- and long-term impacts of hepatic ischemia reperfusion injury post liver transplantation [J]. *Int J Mol Sci*, 2021, **22**(15): 8210.

[6] Capelletti MM, Manceau H, Puy H, *et al*. Ferroptosis in liver diseases: an overview [J]. *Int J Mol Sci*, 2020, **21**(14): 4908.

[7] Yan HF, Tuo QZ, Yin QZ, *et al*. The hepathological role of ferroptosis in ischemia/reperfusion-related injury [J]. *Zool Res*, 2020, **41**(3): 220-230.

[8] Liang DG, Minikes AM, Jiang XJ. Ferroptosis at the intersection of lipid metabolism and cellular signaling [J]. *Mol Cell*, 2022, **82**(12): 2215-2227.

[9] Chen H, Zhao WS, Yan XZ, *et al*. Overexpression of hepcidin alleviates steatohepatitis and fibrosis in a diet-induced nonalcoholic steatohepatitis [J]. *J Clin Translat Hepatol*, 2022, **10**(4): 577-588.

[10] Xin YJ, Gao H, Wang J, *et al*. Manganese transporter Slc39a14 deficiency revealed its key role in maintaining manganese homeostasis in mice [J]. *Cell Discov*, 2017, **18**(3): 17025.

[11] Sun X, Ou Z, Xie M, *et al*. HSPB1 as a novel regulator of ferroptotic cancer cell death [J]. *Oncogene*, 2015, **34**(45): 5617-5625.

[12] Zhang RX, Li MX, Jia ZP. *Rehmannia glutinosa*: review of botany, chemistry and pharmacology [J]. *J Ethnopharmacol*, 2008, **117**(2): 199-214.

[13] Wu PS, Wu SJ, Tsai YH, *et al*. Hot water extracted *Lycium barbarum* and *Rehmannia glutinosa* inhibit liver inflammation and fibrosis in rats [J]. *Am J Chin Med*, 2011, **39**(6): 1173-1191.

[14] Xu J, Wu J, Zhu LY, *et al*. Simultaneous determination of iridoid glycosides, phenethylalcohol glycosides and furfural derivatives in Rehmanniae Radix by high performance liquid chromatography coupled with triple-quadrupole mass spectrometry [J]. *Food Chem*, 2012, **135**(4): 2277-2286.

[15] Perry B, Zhang J, Saleh T, *et al*. Liuwei Dihuang, a traditional Chinese herbal formula, suppresses chronic inflammation and oxidative stress in obese rats [J]. *J Integr Med*, 2014, **12**(5): 447-454.

[16] Charlebois E, Pantopoulos K. Iron overload inhibits BMP/SMAD and IL-6/STAT3 signaling to hepcidin in cultured hepatocytes [J]. *PLoS One*, 2021, **16**(6): e0253475.

[17] Zhou F, Ding M, Gu Y, *et al*. Aurantio-obtusin attenuates non-alcoholic fatty liver disease through AMPK-mediated autophagy and fatty acid oxidation pathways [J]. *Front Pharmacol*, 2021, **12**: 826628.

[18] Wang K, Zhang Z, Tsai HI, *et al*. Branched-chain amino acid aminotransferase 2 regulates ferroptotic cell death in cancer cells [J]. *Cell Death Differ*, 2021, **28**(4): 1222-1236.

[19] Liu GZ, Xu XW, Tao SH, *et al*. HBx facilitates ferroptosis in acute liver failure *via* EZH2 mediated SLC7A11 suppression [J]. *J Biomed Sci*, 2021, **28**(1): 67.

[20] Guo Y, Yang C, Guo R, *et al*. CHOP regulates endoplasmic reticulum stress-mediated hepatoxicity induced by monocrotaline [J]. *Front Pharmacol*, 2021, **12**: 685895.

[21] L, X, Ge J, Li Y, *et al*. Integrative lipidomic and transcriptomic study unravels the therapeutic effects of saikosaponins A and D on non-alcoholic fatty liver disease [J]. *Acta Pharm Sin B*, 2021, **11**(11): 3527-3541.

[22] Li YJ, Liu RP, Ding MN, *et al*. Tetramethylpyrazine prevents liver fibrotic injury in mice by targeting hepatocyte-derived and mitochondrial DNA-enriched extracellular vesicles [J]. *Acta Pharm Sin*, 2022, **43**(8): 2026-2041.

[23] Wu J, Zhou F, Fan G, *et al*. Ferulic acid ameliorates acetaminophen-induced acute liver injury by promoting AMPK-mediated protective autophagy [J]. *IUBMB Life*, 2022, **74**(9): 880-895.

[24] Chen X, Kang R, Kroemer G, *et al*. Broadening horizons: the role of ferroptosis in cancer [J]. *Nat Rev Clin Oncol*, 2021, **18**(5): 280-296.

[25] Zhang Z, Tang J, Song J, *et al*. Elabela alleviates ferroptosis, myocardial remodeling, fibrosis and heart dysfunction in hypertensive mice by modulating the IL-6/STAT3/GPX4 signaling [J]. *Free Rad Biol Med*, 2022, **181**: 130-142.

[26] Cui Y, Zhang Y, Zhao X, *et al*. ACSL4 exacerbates ischemic stroke by promoting ferroptosis-induced brain injury and neuroinflammation [J]. *Brain Behav Immun*, 2021, **93**: 312-321.

[27] Wang Y, Zhang M, Bi R, *et al*. ACSL4 deficiency confers protection against ferroptosis-mediated acute kidney injury [J]. *Redox Biol*, 2022, **51**: 102262.

[28] Jiang X, Stockwell BR, Conrad M. Ferroptosis: mechanisms, biology and role in disease [J]. *Nat Rev Mol Cell Biol*, 2021, **22**(4): 266-282.

[29] Yamada N, Karasawa T, Wakiya T, *et al*. Iron overload as a risk factor for hepatic ischemia-reperfusion injury in liver transplantation: potential role of ferroptosis [J]. *Am J Transplant*, 2020, **20**(6): 1606-1618.
[30] Yang L, Wang H, Yang X, *et al*. Auranofin mitigates systemic iron overload and induces ferroptosis *via* distinct mechanisms [J]. *Signal Transduct Tar*, 2020, **5**(1): 138.
[31] Cheng K, Huang Y, Wang C. 1,25$(OH)_2D_3$ inhibited ferroptosis in Zebrafish liver cells (ZFL) by regulating Keap1-Nrf2-GPx4 and NF-*κ*B-hepcidin axis [J]. *Int J Mol Sci*, 2021, **22**(21): 11334.
[32] Yu Y, Jiang L, Wang H, *et al*. Hepatic transferrin plays a role in systemic iron homeostasis and liver ferroptosis [J]. *Blood*, 2020, **136**(6): 726-739.
[33] Eum HA, Lee WY, Kim SH, *et al*. Anti-inflammatory activity of CML-1: an herbal formulation [J]. *Am J Chin Med*, 2005, **33**(1): 29-40.
[34] Alipieva K, Korkina L, Orhan IE, *et al*. Verbascoside--a review of its occurrence, (bio)synthesis and pharmacological significance [J]. *Biotechnol Adv*, 2014, **32**(6): 1065-1076.
[35] Chen Q, Qi X, Zhang W, *et al*. Catalpol inhibits macrophage polarization and prevents postmenopausal atherosclerosis through regulating estrogen receptor alpha [J]. *Front Pharmacol*, 2021, **12**: 655081.
[36] Tang G, Xu Y, Zhang C, *et al*. Green tea and epigallocatechin gallate (EGCG) for the management of nonalcoholic fatty liver diseases (NAFLD): insights into the role of oxidative stress and antioxidant mechanism [J]. *Antioxidants (Basel, Switzerland)*, 2021, **10**(7): 10071076.
[37] Zwolak I. Epigallocatechin gallate for management of heavy metal-induced oxidative stress: mechanisms of action, efficacy, and concerns [J]. *Int J Mol Sci*, 2021, **22**(8): 22084027.
[38] Conrad M, Proneth B. Broken hearts: iron overload, ferroptosis and cardiomyopathy [J]. *Cell Res*, 2019, **29**(4): 263-264.
[39] Mancias JD, Wang X, Gygi SP, *et al*. Quantitative proteomics identifies NCOA4 as the cargo receptor mediating ferritinophagy [J]. *Nature*, 2014, **509**(7498): 105-109.

Cite this article as: ZHANG Yinhao, JIA Kexin, LI Yufei, *et al*. Rehmanniae Radix Praeparata aqueous extract improves hepatic ischemia/reperfusion injury by restoring intracellular iron homeostasis [J]. *Chin J Nat Med*, 2024, **22**(9): 769-784.

Dr. LI Xiaojiaoyang, professor of School of Life Sciences from Beijing University of Chinese Medicine. She received her PhD from China Pharmaceutical University and Virginia Commonwealth University. Her research interests are the prevention and treatment of chronic liver diseases by traditional Chinese medicine, and committed to exploring the mechanism of chronic digestive disease etiology as well as the development of new drug targets of Chinese medicine origin. Nearly 100 papers have been published in top journals within the field, including *Hepatology, Theranostics, Adv healthc Mater, APSB, Pharmacol Res, APS, iMeta, Chin Herb Med and Chin J Nat Med*. She has been selected as the leader of the key discipline of Chinese medicine of the State Administration of Traditional Chinese Medicine for high level Chinese medicine.